Dynamical Phase Transitions and Instabilities in Open Atomic Many-Body Systems

Sebastian Diehl,[1,2] Andrea Tomadin,[2,3] Andrea Micheli,[1,2] Rosario Fazio,[3] and Peter Zoller[1,2]

[1] *Institute for Theoretical Physics, University of Innsbruck, Technikerstr. 25, A-6020 Innsbruck, Austria*

[2] *Institute for Quantum Optics and Quantum Information of the Austrian Academy of Sciences, A-6020 Innsbruck, Austria*

[3] *NEST, Scuola Normale Superiore and Istituto Nanoscienze - CNR, Pisa, Italy*

We discuss an open driven-dissipative many-body system, in which the competition of unitary Hamiltonian and dissipative Liouvillian dynamics leads to a nonequilibrium phase transition. It shares features of a quantum phase transition in that it is interaction driven, and of a classical phase transition, in that the ordered phase is continuously connected to a thermal state. Within a generalized Gutzwiller approach which includes the description of mixed state density matrices, we characterize the complete phase diagram and the critical behavior at the phase transition approached as a function of time. We find a novel fluctuation induced dynamical instability, which occurs at long wavelength as a consequence of a subtle dissipative renormalization effect on the speed of sound.

PACS numbers: 64.70.Tg,03.75.Kk,67.85.Hj

Experiments with cold atoms provide a unique setting to study nonequilibrium phenomena and dynamics, both in closed systems but also for (driven) open quantum dynamics. This relies on the ability to control the many-body dynamics and to prepare initial states far from the ground state. For closed systems we have seen a plethora of studies of quench dynamics [1, 2], thermalization [3, 4], and transport [5], and also dynamical studies of crossing in a finite time quantum critical points in the spirit of the Kibble-Zurek mechanism [6, 7]. On the other hand, cold atom systems allow to engineer the coupling to an environment and the controlled realization of open driven-dissipative dynamics of many-body systems similarly to studies in quantum optics and mesoscopic physics [8, 9].

For a many-body system in thermodynamic equilibrium the competition of two noncommuting parts of a microscopic Hamiltonian $H = H_1 + gH_2$ manifests itself as a quantum phase transition (QPT), if the ground states for $g \ll g_c$ and $g \gg g_c$ have different symmetries [10]. For temperature $T = 0$ the critical value g_c then separates two distinct quantum phases, while for finite temperature this defines a quantum critical region around g_c in a T vs. g phase diagram. A seminal example in the context of cold atoms in optical lattices is the superfluid–Mott insulator transition in the Bose-Hubbard (BH) model, with Hamiltonian

$$H = -J \sum_{\langle \ell,\ell' \rangle} b_\ell^\dagger b_{\ell'} - \mu \sum_\ell \hat{n}_\ell + \tfrac{1}{2} U \sum_\ell \hat{n}_\ell (\hat{n}_\ell - 1) \ , \quad (1)$$

with b_ℓ bosonic operators annihilating a particle on site ℓ, $\hat{n}_\ell = b_\ell^\dagger b_\ell$ number operators, J the hopping amplitude, and U the onsite interaction strength. For a given chemical potential μ, chosen to fix a mean particle density n, the critical coupling strength $g_c = (U/Jz)_c$ separates a superfluid $Jz \gg U$ from a Mott insulator regime $Jz \ll U$ (z the lattice coordination number).

In contrast, we consider a nonequilibrium situation in which the competition of microscopic quantum mechanical operators results from an interplay of unitary (Hamiltonian) and dissipative (Liouvillian) dynamics. We study cold atom evolution described by a master equation for the many-body density operator

$$\begin{aligned} \partial_t \rho &= -i[H,\rho] + \mathcal{L}[\rho] \ , \quad (2) \\ \mathcal{L}[\rho] &= \frac{1}{2}\kappa \sum_{\langle \ell,\ell' \rangle} \Big(2 c_{\ell\ell'} \rho c_{\ell\ell'}^\dagger - c_{\ell\ell'}^\dagger c_{\ell\ell'} \rho - \rho c_{\ell\ell'}^\dagger c_{\ell\ell'} \Big) \ , \end{aligned}$$

where $c_{\ell\ell'} = (b_\ell^\dagger + b_{\ell'}^\dagger)(b_\ell - b_{\ell'})$ are Lindblad "jump operators" acting on adjacent sites $\langle \ell, \ell' \rangle$. The energy scale κ is the dissipative rate. As shown in [11], such dissipative reservoir couplings can be engineered in a setup where laser driven atoms are coupled to a phonon bath provided by a second condensate. If $J = U = 0$, the Liouvillian drives the system into a pure Bose-Einstein condensate (BEC) steady state independently of the initial state [11]. This can be easily understood in momentum space, where the annihilation part of $c_{\ell\ell'}$ reads $\sum_\lambda (1 - \exp(i\mathbf{q}_\lambda a)) b_\mathbf{q}$, with λ the reciprocal lattice directions and a the lattice constant. $c_{\ell\ell'}$ thus feature a (unique) dissipative zero mode at $\mathbf{q} = 0$ – a many-body "dark state" $|\mathrm{BEC}\rangle \sim b_{\mathbf{q}=0}^{\dagger\, N} |\mathrm{vac}\rangle$, into which the system is consequently driven for long wait times. We stress that it is the *driven* nature of $\mathcal{L}$ that allows to approach a zero entropy state, similarly to laser cooling [12]. This places the system far away from thermodynamic equilibrium.

A purely kinetic Hamiltonian has $|\mathrm{BEC}\rangle$ as an eigenstate, making J an energy scale compatible with dissipation κ. However, an onsite interaction U suppresses off-diagonal order and consequently competes with κ. We therefore obtain a nonequilibrium analog to the conventional purely Hamiltonian scenario, in which the competition of unitary and dissipative dynamics is described by the parameter $u = U/(4\kappa z)$. Dominant dissipation $u \ll 1$ has a superfluid steady state, while dominant interaction $u \gg 1$ results in a diagonal density matrix.

Our scenario bears some resemblance to a system of Josephson junction arrays coupled to a dissipative bath [13], which suitably chosen can stabilize the supercon-

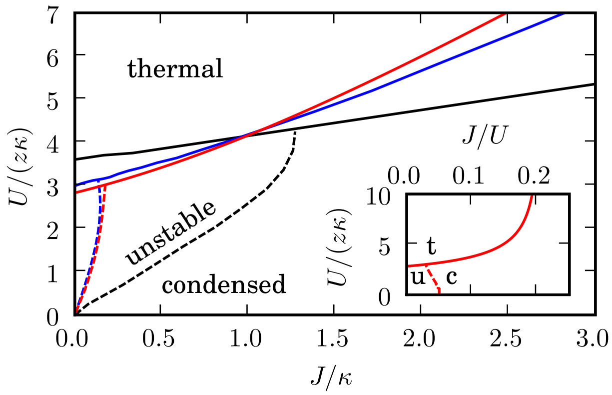

FIG. 1: (color online) Nonequilibrium phase diagram for the model in Eq. (3). The solid lines indicate the border of the dynamical quantum phase transition from a condensed to a homogeneous thermal steady state. The dashed lines delimit the region where the condensed state is stable with respect to spatial fluctuations. The black (blue) lines are the numerical results corresponding to average density $n = 1.0$ ($n = 0.1$). The red line corresponds to the analytical results for $n = 0.1$.

ducting ordered phase. However, a profound difference emerges from that fact that there, the system plus bath is in global thermodynamic equilibrium and the associated phase transitions (thermal or quantum) are equilibrium ones. In the present case the phase diagram has a truly nonequilibrium nature, being entirely due to the driven-dissipative dynamics dictated by Eq. (3).

Our main results are summarized in the complete nonequilibrium steady state phase diagram in Fig. 1. It features a strong coupling phase transition as a function of u, occuring at $u_c = 1/\sqrt{2}$ for $n, J \to 0$. The transition shares features of a QPT in that it is interaction driven, and of a classical phase transition in that the ordered phase terminates in a thermal state, in which the thermal bath is intrinsic, its role played by the occupation of neighbouring sites. Furthermore, we show the existence of a novel dynamical instability that occurs for long enough wait times $\sim (Un)^{-1}$. Its origin is traced back to a subtle renormalization effect of the speed of sound at low energies, which in turn is due to an interplay of short time quantum and long wavelength classical fluctuations. The instability is suppressed by increasing the compatible energy scale J, but it persists at arbitrarily weak interaction parameters Un due to its fluctuation driven nature. This is in marked contrast to the "classical" nonequilibrium dynamical instabilities of condensates in boosted lattices [14, 15] or in exciton-polariton systems [16], which can be induced by external tuning of parameters beyond finite critical values.

Nonlinear mean field master equation.—In order to solve the master equation we have developed a generalized Gutzwiller approach, expected to hold in sufficiently high spatial dimension, which compared to the standard mean field procedure allows to include density matrices corresponding to mixed states. This is implemented by a product ansatz $\rho = \bigotimes_\ell \rho_\ell$ for the full density matrix, with the reduced local density operators $\rho_\ell = \mathrm{Tr}_{\neq \ell}\, \rho$ obtained by tracing out all the degrees of freedom but those on the ℓth site. The equation of motion (EoM) for the reduced density operator reads

$$\partial_t \rho_\ell = -i[h_\ell, \rho_\ell] + \mathcal{L}_\ell[\rho_\ell] \;, \tag{3}$$

with the local Hamiltonian $h_\ell = -J\sum_{\langle \ell' | \ell\rangle}(\langle b_{\ell'}\rangle b_\ell^\dagger + \langle b_{\ell'}^\dagger\rangle b_\ell) - \mu \hat{n}_\ell + \frac{1}{2}U\hat{n}_\ell(\hat{n}_\ell - 1)$ reproducing the standard form of the Gutzwiller mean field approximation and a Liouvillian of the form $\mathcal{L}_\ell[\rho_\ell] = \kappa\sum_{\langle \ell'|\ell\rangle}\sum_{r,s=1}^{4}\Gamma_{\ell'}^{rs}[2A_\ell^r\rho_\ell A_\ell^{s\dagger} - A_\ell^{s\dagger}A_\ell^r\rho_\ell - \rho_\ell A_\ell^{s\dagger}A_\ell^r]$. The Liouvillian is constructed with the vector of operators $\mathbf{A}_\ell = (1, b_\ell^\dagger, b_\ell, \hat{n}_\ell)$ and the matrix of correlation functions $\Gamma_\ell^{r,s} = \sigma^r\sigma^s \mathrm{Tr}_\ell A_\ell^{(5-s)\dagger}A_\ell^{(5-r)}\rho_\ell$, for $\sigma = (-1,-1,1,1)$. The ρ-dependent correlation matrix makes the master equation *nonlinear* in ρ_ℓ.

Dynamical quantum phase transition.—At $U = 0$ a steady state solution of Eq. (3) is given by the pure state $\rho_\ell^{(c)} = |\Psi\rangle\langle\Psi|$ for any ℓ together with the choice $\mu = -Jz$, where $|\Psi\rangle$ is a coherent state of parameter $ne^{i\theta}$ for any phase θ [17]. In order to understand the effect of a finite interaction U, we apply the rotating-frame transformation $\hat{V}(U) = \exp[iU\hat{n}_\ell(\hat{n}_\ell - 1)t]$ to Eq. (3). This removes the interaction term from the unitary evolution, but the annihilation operators become $\hat{V}b_\ell\hat{V}^{-1} = \sum_m \exp(imUt)|m\rangle_\ell\langle m|b_\ell$. The effect of a finite U is thus to rotate the phase of each Fock state differently, leading to dephasing of the coherent state $\rho_\ell^{(c)}$. Hence, for strong enough U, off-diagonal order is suppressed completely and the density matrix becomes diagonal. In this case Eq. (3) reduces precisely to the master equation for a system of bosons coupled to a thermal reservoir with occupation n [17], whose solution is a mixed diagonal thermal state $\rho^{(t)}$. Interestingly, unlike the standard case of an external heat bath, the strongly interacting system provides its own heat reservoir.

We substantiate the discussion above with the numerical integration of the EoM (3) for a homogeneous system (we drop the index ℓ). The system is initially in the coherent state and the condensate fraction $|\psi|^2/n$, where $\psi = \langle b\rangle$, decreases in time depending on the value of the interaction strength U. The result is a continuous transition from the coherent state $\rho^{(c)}$ to the thermal state $\rho^{(t)}$, shown in Fig. 2 for some typical parameters. The boundary between the thermal and the condensed phase with varying J, n is shown in Fig. 1 with solid lines.

The transition is a smooth crossover for any finite time, but for $t \to \infty$ a sharp nonanalytic point indicating a second order phase transition develops. In the universal vicinity of the critical point, $1/\kappa t$ may be viewed as an irrelevant coupling in the sense of the renormalization group. We may use this attractive irrelevant direction to extract the critical exponent α for the order parameter

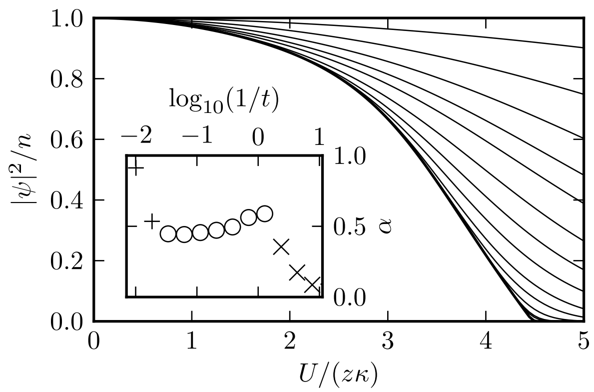

FIG. 2: Stroboscopic plot of the time evolution of the condensate fraction as a function of the interaction strength U, for $J = 1.5\,\kappa$ and $n = 1$. For large times it converges to the lower thick solid line. The critical point is $U_c \simeq 4.5\,\kappa z$. Inset: Near critical evolution reflected by the logarithmic derivative of the order parameter $\psi(t)$, for $J = 0$, $n = 1$, and $U \lesssim U_c$. The early exponential decay ($\times$) is followed by a scaling regime ($\circ$) with exponent $\alpha \simeq 0.5$. The final exponential runaway ($+$) is due to a small deviation from the critical point.

from the scaling solution $|\psi(t)| \propto (\kappa t)^{-\alpha}$. In the inset of Fig. 2 we plot $\alpha(t) = d\log(\psi)/d\log(1/t)$ and read off the critical exponent $\alpha = 0.5$ in the scaling regime, which is an expected result given the mean field nature of the Gutzwiller ansatz.

Low-density limit.—In the low density limit $n \ll 1$ we obtain an analytical understanding of the time evolution based on the observation that the six correlation functions ψ, $\langle b_\ell^2\rangle$, $\langle b_\ell^\dagger b_\ell^2\rangle$, and complex conjugates, form a closed (nonlinear) subset which decouples from the *a priori* infinite hierarchy of normal ordered correlation functions $\langle b_\ell^{\dagger n} b_\ell^m\rangle$. We first use this result to obtain analytically the critical exponent α discussed above. For a homogeneous system with $J = 0$ the EoMs read

$$\begin{aligned} \partial_t\psi &= i\mu\psi + (-iU + 4\kappa)\langle b^\dagger b^2\rangle - 4\kappa\psi^*\langle b^2\rangle\ , \\ \partial_t\langle b^\dagger b^2\rangle &= 8n\kappa\psi + (-iU + i\mu - 8\kappa)\langle b^\dagger b^2\rangle\ , \\ \partial_t\langle b^2\rangle &= (-iU + 2i\mu - 8\kappa)\langle b^2\rangle + 8\kappa\psi^2\ . \end{aligned} \quad (4)$$

The structure of the equations suggest that $\langle b^2\rangle$ decays much faster than the other correlations for $U = U_c$, so that we may take $\partial_t\langle b^2\rangle = 0$ and hence $\langle b^2\rangle \propto \psi^2$. At the critical point the two linear contributions to $\partial_t\psi$ vanish due to the zero mass eigenvalue at criticality and $\partial_t\psi \propto \kappa\psi^2\psi^*$. It follows that $|\psi| \simeq 1/(4\sqrt{\kappa t})$ in agreement with the numerical result in Fig. 2.

To study the interaction induced depletion of the condensate fraction, it is convenient to use "connected" correlation functions, built with the fluctuation operator $\delta b = b - \psi_0$. Here ψ_0 is the constant value of the order parameter in the steady state, and $\langle\delta b\rangle = 0$. From (4) we obtain a closed *linear* system of EoMs, if ψ_0 is considered as a parameter, determined self-consistently from the identity $n = \langle\delta b^\dagger\delta b\rangle + |\psi_0|^2$. The value of the chemical potential is fixed to remove the driving terms in the equations for $\langle\delta b\rangle$, leading to $\mu = nU$. This is an equilibrium condition similar to the vanishing of the mass of the Goldstone mode in a thermodynamic equilibrium system with spontaneous symmetry breaking. The solution of the equations in steady state yields the condensate fraction

$$\frac{|\psi_0|^2}{n} = 1 - \frac{2u^2\left(1 + (j+u)^2\right)}{1 + u^2 + j(8u + 6j\left(1 + 2u^2\right) + 24j^2u + 8j^3)}\ , \quad (5)$$

with dimensionless variable $j = J/(4\kappa)$. Eq. (5) reduces to the simple quadratic expression $1 - 2u^2$ in the limit of zero hopping, with the critical point $U_c(J = 0) = 4\kappa z/\sqrt{2}$. The phase boundary, obtained by setting $\psi_0 = 0$ in Eq. (5), reads $u_c = j + \sqrt{1/2 + 2j^2}$. Fig. 1 shows that these compact analytical results (solid red line) match the full numerics for small densities (solid blue line), and also explain the qualitative features of the phase boundary for large densities. We note the absence of distinct commensurability effects for e.g. $n = 1$, tied to the fact that the interaction also plays the role of heating.

Dynamical instability.—Numerically integrating the full EoM (3) with site-dependence (in one dimension for simplicity), we observe a dynamical instability, manifesting itself at late times in a long wavelength density wave with growing amplitude, cf. Fig. 3 (a). Numerical linearization of Eq. (3) around the homogeneous steady state allows to draw a phase border for the unstable phase (see Fig. 1). The instability is cured by the increase of hopping J, which is associated to an operator compatible with dissipation κ. Furthermore, we note that the thermal state is always dynamically stable against long wavelength perturbations.

The origin of this instability is intriguing and we discuss it analytically within the low-density limit introduced above. We linearize in time the EoM (3), writing the generic connected correlation function as $\langle\hat{O}_\ell\rangle(t) = \langle\hat{O}_\ell\rangle_0 + \delta\langle\hat{O}_\ell\rangle(t)$, where $\langle\hat{O}_\ell\rangle_0$ is evaluated on the homogeneous steady state of the system. The EoM for the time and space dependent fluctuations is then Fourier transformed, resulting in a 7×7 matrix evolution equation $\partial_t\delta\Phi_{\mathbf{q}} = M\delta\Phi_{\mathbf{q}}$ for the correlation functions $\Phi_{\mathbf{q}} = (\langle\delta b\rangle_{\mathbf{q}}, \langle\delta b^\dagger\rangle_{\mathbf{q}}, \langle\delta b^\dagger\delta b\rangle_{\mathbf{q}}, \langle\delta b^2\rangle_{\mathbf{q}}, \langle\delta b^{\dagger 2}\rangle_{\mathbf{q}}, \langle\delta b^\dagger\delta b^2\rangle_{\mathbf{q}}, \langle\delta b^{\dagger 2}\delta b\rangle_{\mathbf{q}})$. We note that the fluctuation $\delta\langle\delta b\rangle_{\mathbf{q}}$ ($\delta\langle\delta b^\dagger\rangle_{\mathbf{q}}$) coincides with the fluctuation of the order parameter $\delta\psi_{\mathbf{q}}$ ($\delta\psi^*_{-\mathbf{q}}$). The full matrix M can be easily diagonalized numerically revealing the spectrum in Fig. 3 (we display only the relevant real part γ corresponding to damping). The lowest-lying branch gives $\gamma_{\mathbf{q}} < 0$ in a small interval around the origin $\mathbf{q} = 0$. This means that the correlation functions grow exponentially $\propto e^{\gamma t}$ in a range of low momenta, resulting e.g. in a long wavelength density wave like in Fig. 3 (a).

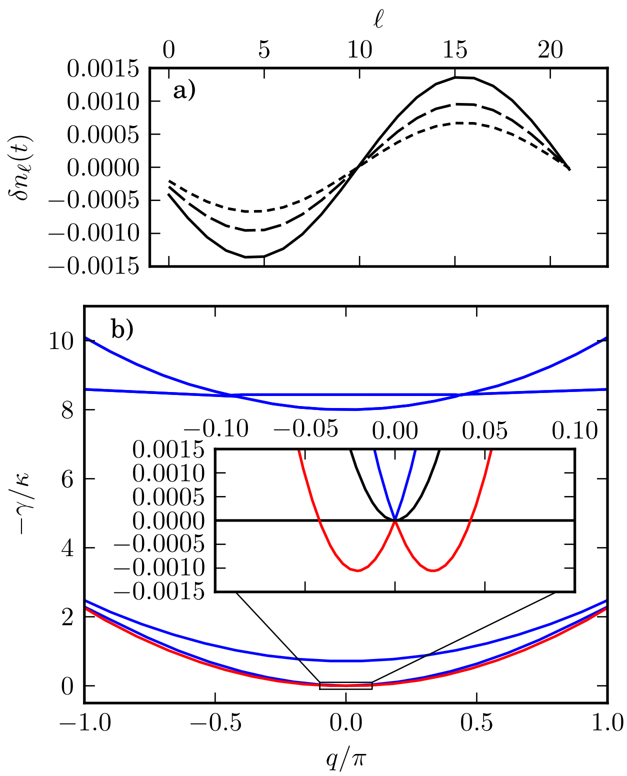

FIG. 3: (color online) (a) The growing spatial fluctuation $\delta n_\ell = n_\ell - n$ for $U = 3.0\,\kappa$, $J = 0$, and $n = 1.0$. A lattice with 22 sites and periodic boundary conditions has been used and three instants in time are shown. (b) Real (dissipative) part of the spectrum $\gamma_{\mathbf{q}}$ from the analytical low density limit for $J = 0$, $n = 0.1$, and $U = 1.0\,\kappa$. The inset magnifies the parameter region with unstable modes (red solid line). The black solid line is the bare dissipative spectrum $\kappa_{\mathbf{q}}$.

Due to the scale separation for $\mathbf{q} \to 0$ in the matrix M apparent from Fig. 3 (b), we can apply second order perturbation theory twice in a row to integrate out the fast modes $\gamma \propto \kappa$ and $\propto \kappa n$. We then obtain an effective low energy EoM for the fluctuations of the order parameter $(\delta\psi_{\mathbf{q}}, \delta\psi^*_{-\mathbf{q}})$, governed by a 2×2 matrix

$$M_{\rm eff} = \begin{pmatrix} Un + \epsilon_{\mathbf{q}} - i\kappa_{\mathbf{q}} & Un + 9un\kappa_{\mathbf{q}} \\ -Un - 9un\kappa_{\mathbf{q}} & -Un - \epsilon_{\mathbf{q}} - i\kappa_{\mathbf{q}} \end{pmatrix}, \qquad (6)$$

where $\epsilon_{\mathbf{q}} = J\mathbf{q}^2$ represents the kinetic contribution and $\kappa_{\mathbf{q}} = 2(2n+1)\kappa\mathbf{q}^2$ is the bare dissipative spectrum. The form of the EoM reflects the structure of the spatial fluctuations which are included in our approach, that may be understood as scattering off the mean fields in opposite directions. We note that a naive *a priori* restriction to the 2×2 set corresponding to the subset $(\delta\psi_\ell, \delta\psi^*_\ell)$ would be inconsistent, for example destroying the dark state property present in the correct solution $M_{\rm eff}$. On the other hand, factorizing the correlation functions in the Liouvillian $\mathcal{L}_\ell$ yields a dissipative Gross-Pitaevski equation but its linearization in time produces a matrix $M_{\rm eff}$ *without* the fluctuation induced term $\sim u$ and fails to describe the dynamical instability. Thus, in order to correctly capture the physics of the instability at long wavelength $\mathbf{q} \to 0$, the onsite quantum correlations renormalizing $M_{\rm eff}$ have to be properly taken into account.

We can make the nature of the instability even more transparent from calculating the lowest eigenvalue of $M_{\rm eff}$, $\gamma_{\mathbf{q}} \simeq {\rm i}c|\mathbf{q}| + \kappa_{\mathbf{q}}$, with speed of sound $c = \sqrt{2Un[J - 9Un/(2z)]}$. If the hopping amplitude is smaller than the critical value $J_{\rm c} = 9Un/(2z)$ the speed of sound turns imaginary and contributes to the dissipative real part of $\gamma_{\mathbf{q}}$. The nonanalytic renormalization contribution $\sim |\mathbf{q}|$ always dominates the bare quadratic piece for low momenta, explaining the shape in the inset of Fig. 3 and rendering the system unstable. The linear slope of the stability border for small J and U is clearly visible from the numerical results in Fig. 1.

Conclusion.—We have discussed the steady state phase diagram resulting from a competition of unitary Bose-Hubbard and dissipative dynamics with dark state. The features found in the present model are expected to be generic and representative for a whole class of nonequilibrium models discussed recently in the context of reservoir engineering and dissipative preparation of given long range ordered entangled states of qubits or spins on a lattice [18, 19] and paired fermions [11, 20]. In particular, we emphasize the importance of a compatible energy term for the achievement of stability of driven-dissipative many-body systems in future experiments.

We thank M. Hayn, A. Pelster, S. Kehrein, M. Möckel, and J. V. Porto for interesting discussions. This work was supported by the Austrian Science Foundation through SFB FOQUS, SCALA and by EU Networks. The plots have been produced with the Open Source scipy/numpy/matplotlib packages of the Python programming language.

[1] P. Calabrese and J. Cardy, Phys. Rev. Lett. **96**, 136801 (2006); C. Kollath, A. M. Läuchli, and E. Altman, *ibid.* **98**, 180601 (2007); A. Silva, *ibid.* **101**, 120603 (2008); M. Möckel and S. Kehrein, *ibid.* **100**, 175702 (2008).

[2] M. Greiner, O. Mandel, T.W. Hänsch, and I. Bloch, Nature **419**, 51 (2002); B. Paredes *et al.*, *ibid.* **429**, 277 (2004); L.E. Sadler *et al.*, *ibid.* **443**, 312 (2006).

[3] M. Cramer, C.M. Dawson, J. Eisert, and T.J. Osborne, Phys. Rev. Lett. **100**, 030602 (2008); M. Rigol, V. Dunjko, and M. Olshanii, Nature **452**, 854 (2008); G. Roux, Phys. Rev. A **79**, 021608(R) (2009); L.C. Venuti and P. Zanardi, arXiv:0912.3357.

[4] T. Kinoshita, T. Wenger, and D.S. Weiss, Nature **440**, 900 (2006); S. Hofferberth *et al.*, Nature Phys. **4**, 489 (2008).

[5] S. Montangero, R. Fazio, P. Zoller, and G. Pupillo, Phys. Rev. A **79**, 041602(R) (2009); J. Schachenmayer, G. Pupillo, and A.J. Daley, New J. Phys. **12**, 025014 (2010).

[6] K. Sengupta, S. Powell, and S. Sachdev, Phys. Rev. A **69**, 053616 (2004); W.H. Zurek, U. Dorner, and P. Zoller, Phys. Rev. Lett. **95**, 105701 (2005); T. Prosen and I. Pizorn, *ibid.* **101**, 105701 (2008); C. De Grandi, V. Gritsev and A. Polkovnikov, arXiv:0909.5181; R.A. Barankov, arXiv:0910.0255.

[7] C.N. Weiler *et al.*, Nature **455**, 948 (2008).

[8] S.A. Moskalenko and D.W. Snoke, *Bose-Einstein Condensation of Excitons and Biexcitons*, Cambridge Univ. Press, Cambridge (2000); J. Keeling, F.M. Marchetti, M.H. Szymanska, and P.B. Littlewood, Semicond. Sci. Technol. **22**, R1 (2007).

[9] E.G. Dalla Torre, E. Demler, T. Giamarchi, and E. Altman, arXiv:0908.0868.

[10] S. Sachdev, *Quantum Phase Transitions*, Cambridge Univ. Press, Cambridge (1999).

[11] S. Diehl *et al.*, Nature Phys. **4**, 1073 (2008); B. Kraus *et al.*, Phys. Rev. A **78**, 042307 (2008).

[12] A. Aspect *et al.*, Phys. Rev. Lett. **61**, 826 (1988); M. Kasevich and S. Chu, *ibid.* **69**, 1741 (1992).

[13] A. Schmid, Phys. Rev. Lett. **51**, 1506 (1983); S. Chakravarty, G.-L. Ingold, S. Kivelson, and A. Luther, *ibid.* **56**, 2303 (1986); A. Kampf and G. Schön, Phys. Rev. B **36**, 3651 (1987); S. Chakravarty, S. Kivelson, G.T. Zimanyi, and B.I. Halperin, *ibid.* **35**, 7256 (1987); R. Fazio and H. van der Zant, Phys. Rep. **355**, 235 (2001).

[14] B. Wu and Q. Niu, Phys. Rev. A **64**, 061603(R) (2001); A. Smerzi, A. Trombettoni, P.G. Kevrekidis, and A.R. Bishop, Phys. Rev. Lett. **89**, 170402 (2002); E. Altman *et al.*, *ibid.* **95**, 020402 (2005); A. Polkovnikov *et al.*, Phys. Rev. A **71**, 063613 (2005).

[15] S. Burger *et al.*, Phys. Rev. Lett. **86**, 4447 (2001); M. Cristiani *et al.*, Optics Express **12**, 4 (2004); J. Mun *et al.*, Phys. Rev. Lett. **99**, 150604 (2007).

[16] J. Kasprzak *et al.*, Nature **443**, 409 (2006); M. Wouters and I. Carusotto, arXiv:1001.0660.

[17] C.W. Gardiner and P. Zoller, *Quantum Noise* , Springer-Verlag, Berlin (1999).

[18] F. Verstraete, M.M. Wolf, and J.I. Cirac, Nature Phys. **5**, 633 (2009).

[19] H. Weimer *et al.*, arXiv:0907.1657.

[20] W. Yi *et al.*, in preparation (2010).